

Optimal Control For Power-Off Landing Of A Small-Scale Helicopter A Pseudospectral Approach

Skander Taamallah, Xavier Bombois and Paul Van den Hof

Abstract— We derive optimal power-off landing trajectories, for the case of a small-scale helicopter UAV. These open-loop optimal trajectories represent the solution to the minimization of a cost objective, given system dynamics, controls and states equality and inequality constraints. The plant dynamics features a 3-D nonlinear helicopter model, including dynamics from the rigid body, the main rotor Revolutions Per Minute (RPM), and the actuators. The novel part of this paper is threefold. First, we provide a new cost functional which, during the flight, maximizes helicopter performance and control smoothness, while minimizing roll-yaw cross-coupling. Second, and aside from the standard state and control bounds, we provide a trajectory constraint on tail rotor blade tip, to avoid ground strike when the helicopters pitches up, just before touch-down. Third, we apply the pseudospectral collocation discretization scheme, through a direct optimal control method, to solve our problem. The advantage of the pseudospectral method, compared to other direct optimal control approaches, lies in its exponential convergence, implying increased computational efficiency, provided the functions under considerations are sufficiently smooth. Finally, we conclude by a discussion of several simulation examples.

I. INTRODUCTION

Helicopter power-off flight, or autorotation, is a condition in which no power plant torque is applied to the main and tail rotors, a flight condition which is somewhat comparable to gliding for a fixed-wing aircraft. During an autorotation, the main rotor is not driven by a running engine, but by air flowing through the rotor disk bottom-up, while the helicopter is descending. An autorotative flight is entered when the engine fails on a single-engine helicopter, or when a tail rotor failure requires engine shut down. Our goal is to find optimal autorotative trajectories, that maximize flight performance and control smoothness, while minimizing cross-coupling effects. Hence, for a range of initial conditions for which feasible solutions do exist, i.e. in the form of safe landing, optimal autorotative trajectories can be computed off-line by a Trajectory Planner (TP), and stored as lookup tables, on-board a flight control computer. By so doing, these trajectories provide both the optimal states to be tracked by a feedback Trajectory Tracker (TT), and the feedforward nominal controls needed to track the trajectory. In this paper, we present the design of such a TP, in the case of a continuous-time, deterministic, nonlinear,

and constrained framework; solved through a direct optimal control method. Here the continuous-time formulation is first discretized, using a pseudospectral numerical scheme, known to provide exponential convergence, provided the functions under considerations are sufficiently smooth. Pseudospectral techniques have widely been used in space and launch/reentry applications. However, they have so far only seen limited use in other aeronautical or (helicopter) UAV applications. Next, our problem is transcribed to a NonLinear Programming problem (NLP), and this latter is solved numerically by a well known and efficient optimization technique, in our case a Sequential Quadratic Programming (SQP) method.

Over the last four decades, researchers have addressed the optimal autorotative flight problem through several optimization techniques. We start by mentioning the successful autorotative flight demonstration in the case of a small-scale helicopter, through the use of an apprenticeship learning method [1]. Next, for the case of first principles based models, we briefly review the different optimization strategies that have been researched. Indirect optimal control methods have been employed [2], [3], [4], whereas direct collocation optimal control methods have been explored [5], [6], [7], [8], and a direct multiple shooting optimal control method has been outlined [8]. Aside from these optimal control strategies, three other methods have also been investigated: (i) nonlinear, neural-network augmented, model-predictive control [9], (ii) a parameter optimization scheme, repeatedly solved, to find a backwards reachable set leading to safe landing [10], and (iii) a parameter optimization scheme generating segmented routes, selecting a sequence of straight lines and curves [11], [12].

The most natural framework for addressing trajectory planning problems is through optimal control theory [13]. Besides, any strategy that does not rely on the combined use of both realistic 3-D first principles based models, and optimal control, results at best in sub-optimal solutions, since the full dynamics of the vehicle are neither exploited from a vehicle flight performance viewpoint, nor from a control-optimization viewpoint. Further, for the definition of the cost functional, most of the here-above listed contributions have focused solely upon the minimization of vehicle kinetic energy at the instant of touch-down. Some have considered using a running cost over time, which includes criteria involving either (i) the minimization of control rates [6], [8], or (ii) the minimization of main rotor

Skander Taamallah is with the National Aerospace Laboratory (NLR), Anthony Fokkerweg 2, 1059 CM, Amsterdam, The Netherlands, email: staamall@nlr.nl

Skander Taamallah, Xavier Bombois, Paul Van den Hof are with the Delft Center for Systems and Control, Delft University of Technology, Mekelweg 2, 2628 CD, Delft, The Netherlands, email: {x.j.a.bombois, P.M.J.VandenHof@tudelft.nl}

RPM deviations from its nominal value, while limiting the excessive build-up of vehicle kinetic energy during the descent [7], [4]. None of the previous results have considered the definition of a cost functional that includes all of these criteria, while also adding minimization of vehicle sideways flight, and maximization of flight into the wind. Indeed, this represents the first novel contribution of our paper. The second contribution is characterized by a trajectory constraint on tail rotor blade tip, to avoid ground strike when the helicopters pitches up, just before touch-down. The third is the application of the pseudospectral discretization, to solve our optimal control problem.

The remainder of the paper is organized as follows. In Section II, the general case optimal problem is defined. In Section III, direct optimal control and the pseudospectral method are reviewed. In Section IV, simulation results are analyzed. Finally, conclusions and future directions are presented in Section V.

II. PROBLEM STATEMENT

We consider the following general problem, consisting in minimizing the Bolza cost functional $J(\mathbf{x}(t), \mathbf{u}(t), T_o, T_f)$, with the state vector of the system $\mathbf{x}(t)$, and control input $\mathbf{u}(t)$, both defined on compact sets $\mathbf{x}(t) \in \mathcal{X}(t) \subseteq \mathbb{R}^{n_x}$, $\mathbf{u}(t) \in \mathcal{U}(t, \mathbf{x}(t)) \subseteq \mathbb{R}^{n_u}$, denoting the feasible control and state spaces respectively. Here, for the purpose of generality, the control set $\mathcal{U}(t, \mathbf{x}(t))$ is allowed to be state-dependent to accommodate for considerations of aerospace applications. Further, the independent time variable t is defined over the time domain $\Omega = (T_o, T_f)$, where the final time T_f may be free or fixed.

$$J(\mathbf{x}(t), \mathbf{u}(t), T_o, T_f) \triangleq \Phi(\mathbf{x}(T_o), T_o, \mathbf{x}(T_f), T_f) + \int_{\Omega} \Psi(\mathbf{x}(t), \mathbf{u}(t), t) dt \quad (1)$$

In the general problem formulation, the cost functional J has contributions from a fixed cost $\Phi(\mathbf{x}(T_o), T_o, \mathbf{x}(T_f), T_f)$, and a running cost over time $\int_{\Omega} \Psi(\mathbf{x}(t), \mathbf{u}(t), t) dt$. Additionally, this cost functional J is subject to the system dynamic constraints, where the usual representation is given by a set of Ordinary Differential Equations (ODEs) of the form

$$\dot{\mathbf{x}} = f(\mathbf{x}(t), \mathbf{u}(t), t) \quad t \in \Omega \quad (2)$$

The initial and final-time boundary inequality conditions are given by

$$\begin{aligned} B_o(\mathbf{x}(T_o), \mathbf{u}(T_o), T_o) &\leq 0 \\ B_f(\mathbf{x}(T_f), \mathbf{u}(T_f), T_f) &\leq 0 \end{aligned} \quad (3)$$

Conjointly the algebraic trajectory inequality constraints are given by

$$T(\mathbf{x}(t), \mathbf{u}(t), t) \leq 0 \quad t \in \Omega \quad (4)$$

For generality, the boundary and trajectory constraints (3) (4) have been expressed as inequality constraints, equality constraints can simply be enforced by equating upper and

lower bounds. Further, in (1)-(4) the functions Φ , Ψ , f , B_i , and T are assumed to be sufficiently smooth, i.e. at least C^2 . The solution to the trajectory planning gives the control input, which minimizes the cost functional, while enforcing the constraints

$$\mathbf{u}^*(t) \triangleq \arg \min_{\mathbf{u}(t) \in \mathcal{U}(t, \mathbf{x}(t))} J(\mathbf{x}(t), \mathbf{u}(t), T_o, T_f) \quad (5)$$

For our optimal autorotative trajectory, the following thirteen-state and four-input vectors are considered

$$\begin{aligned} \mathbf{x} &= (x_N \ x_E \ x_Z \ \phi \ \theta \ \psi \ u \ v \ w \\ &\quad p \ q \ r \ \Omega_{MR})^T \\ \mathbf{u} &= (\theta_0 \ \theta_{TR} \ \theta_{1c} \ \theta_{1s})^T \end{aligned} \quad (6)$$

With the ensuing state vector nomenclature: (x_N, x_E, x_Z) represent the 3-D position of the vehicle Center of Gravity (CG), in inertial frame F_I given by (x_I, y_I, z_I) , see Fig. 1; (ϕ, θ, ψ) represent the vehicle angular orientations in roll-pitch-yaw respectively, with respect to F_I ; (u, v, w) and (p, q, r) represent the CG linear and rotational velocities respectively, with respect to F_I , and projected in the helicopter body frame F_b given by (x_b, y_b, z_b) , see Fig. 1; Ω_{MR} represents the Main Rotor (MR) angular velocity, also called MR Revolutions Per Minute (RPM). The control input vector consists of θ_0 , the MR blade collective pitch, primarily controlling vertical helicopter motion and MR RPM; θ_{TR} the Tail Rotor (TR) blade collective pitch, primarily controlling directional (yaw) helicopter motion; θ_{1c} the MR blade lateral cyclic pitch, primarily controlling lateral and roll motion; and finally θ_{1s} the MR blade longitudinal cyclic pitch, primarily controlling longitudinal and pitch motion.

A. Cost Functional

In this paper, we want to find the optimal autorotative trajectory, corresponding to an initial condition for which a feasible solution exists, i.e. the helicopter has the capability to effectuate a safe landing. In this case, the final cost $\Phi(\mathbf{x}(T_f), T_f)$, where in the sequel we drop the cost functional dependency on T_o , may equivalently be replaced by tight bounds, adjusted for safe landing, on the final values of vehicle kinetic energy and attitude angles. Hence, we can set $\Phi(\mathbf{x}(T_f), T_f) = 0$. This in turn simplifies the optimization process, and hence lowers the computational time. Next, the cost functional is defined, from engineering judgment, as a running cost over time s.t.

$$\begin{aligned} J(\mathbf{x}(t), \mathbf{u}(t), T_f) &:= \int_{\Omega} \Psi(\mathbf{x}(t), \mathbf{u}(t), t) dt \\ &= \int_{\Omega} \left[(\dot{\theta}_0^2 + \dot{\theta}_{TR}^2 + \dot{\theta}_{1c}^2 + \dot{\theta}_{1s}^2) \right. \\ &\quad + (\Omega_{MR} - \Omega_{MR_{100\%}})^2 \\ &\quad + (u^2 + w^2) + v^2 \\ &\quad \left. + (\psi - \psi_f)^2 \right] dt \end{aligned} \quad (7)$$

The input rates $(\dot{\theta}_0^2 + \dot{\theta}_{1c}^2 + \dot{\theta}_{1s}^2 + \dot{\theta}_{TR}^2)$ are added to (i) minimize the battery power consumption, and (ii) encourage

smoother control policies, hence avoiding *bang-bang* type solutions, that might excite unmodeled or undesirable high frequency dynamics or resonances.

The term $(\Omega_{MR} - \Omega_{MR_{100\%}})^2$ is added to penalize any large deviations in main rotor speed from its nominal (power-on) value given by $\Omega_{MR_{100\%}}$. Indeed, a rotor over-speed would increase, beyond acceptable values, the structural stresses on the main rotor hub (blade centrifugal stresses) and rotor hinges. On the other hand, a rotor under-speed would be unsafe for the following two reasons: (i) it increases the region of blade stall, increasing rotor drag and decreasing rotor lift, hence resulting in a higher helicopter sink rate, and (ii) it lowers the stored rotor kinetic energy, which is a crucial element for a good landing flare capability.

The term $(u^2 + w^2)$ is added to limit the excessive build-up of vehicle kinetic energy during the descent. Indeed, a high kinetic energy complicates the final maneuver just prior to touchdown, since more energy needs to be dissipated, i.e. the timing of the controls input application becomes increasingly critical.

The term v^2 , generally of low magnitude, is primarily added to limit vehicle sideslip flight, as this latter decreases the flight performance by increasing vehicle drag, and increasing roll-yaw coupling, hence increasing the workload of any feedback Trajectory Tracker (TT) controller.

Finally, ψ_f refers to the wind heading angle known through either on-board measurement or data-uplink, from a ground-based wind sensor. The term $(\psi - \psi_f)^2$ is added to encourage flight and landing into the wind. This enhances flight performance and lowers kinetic energy at touchdown.

B. Helicopter Model

The plant model used here is adapted from the helicopter model presented in [14]. This latter reproduces the flight dynamics of a small-scale helicopter. This nonlinear model includes the twelve-states rigid body equations of motion, and the single-state main rotor RPM, while the higher-order main rotor phenomena are based on their corresponding steady-state expressions.

C. Boundary Conditions

The initial boundary conditions $B_o(\mathbf{x}(T_o), \mathbf{u}(T_o), T_o) \leq 0$ describe the steady-state flight condition, at the instant prior to the autorotative maneuver, whereas the aim of the final boundary conditions $B_f(\mathbf{x}(T_o), \mathbf{u}(T_o), T_o) \leq 0$ is fourfold: (i) set the vehicle on the ground (only a constraint on the z-axis, North and East positions are free), (ii) account for the vehicle's inherent physical limitations (bounds on main rotor RPM), (iii) provide additional tight bounds on the vehicle kinetic energy and attitude angles, in accordance with technical specifications for safe landing, and (iv) check for the actuators range limitations.

D. Trajectory Constraints $T(\mathbf{x}(t), \mathbf{u}(t), t) \leq 0 \quad t \in \Omega$

The goal of the trajectory constraints is also fourfold: (i) account for the vehicle's inherent physical and flight envelope limitations (bounds on speeds, attitude, and main

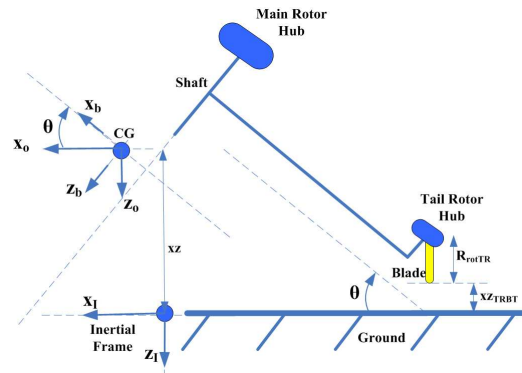


Fig. 1. Tail Rotor Ground Clearance (Longitudinal View)

rotor RPM), (ii) account for environmental constraints (the helicopter cannot descend below ground), (iii) check for the intrinsic actuators dynamic and range limitations, and (iv) avoid ground strike by the tail rotor blade tip, just before touch-down. Here, the tail rotor radius is given by R_{rotTR} , and the smallest distance between the tail rotor blade tip and the ground, see Fig. 1, is given by the distance $x_{Z_{TRBT}}$ in F_I . The F_b position of the tail rotor hub is given by (x_{TR}, y_{TR}, z_{TR}) , hence the lowest 3-D position of the blade tip, for a positive pitch θ , is given in F_b by

$$\mathbf{x}_{TRBT} = \begin{pmatrix} x_{TR} - R_{rotTR} \cdot \sin \theta \\ y_{TR} \\ z_{TR} + R_{rotTR} \cdot \cos \theta \end{pmatrix} \quad (8)$$

Accordingly, the z-axis position of the blade tip in F_I is

$$x_{Z_{TRBT}} = x_Z + \begin{pmatrix} 0 \\ 0 \\ 1 \end{pmatrix}^T \cdot \mathbb{T}_{ob} \cdot \mathbf{x}_{TRBT} \quad (9)$$

With \mathbb{T}_{ob} the transformation matrix from F_b to the vehicle-carried normal earth frame F_o , and x_Z the z-axis position of the CG in F_I . Note that both the z-axis of frames F_o and F_I are oriented positive downwards. Finally, we have $x_{Z_{TRBT}} \leq Z_{safety} \leq 0$, with Z_{safety} a safety margin.

III. DIRECT OPTIMAL CONTROL AND THE PSEUDOSPECTRAL DISCRETIZATION

We solve our problem, through a direct optimal control method. In this context, the continuous-time optimal control problem is first discretized and the problem is transcribed to a NLP, without formulating an alternate set of optimality conditions as done through indirect methods. The resulting NLP can be solved numerically, by well known and efficient optimization techniques, such as SQP methods or Interior Point (IP) methods. These methods in turn attempt to satisfy a set of conditions called the Karush-Kuhn-Tucker (KKT) conditions. Now regarding the discretization of the continuous-time optimal control problem, the three most common approaches are Single-Shooting (SS) [15], Multiple-Shooting (MS) [16], and State and Control Parameterization (SCP) [17]; this latter sometimes known as transcription in the aerospace community, or as simultaneous strategy in the

chemical and process community. Briefly summarized, the advantage of direct SS is that it generates a small number of variables, while its main disadvantage is that a small change in the initial condition can produce a very large change in the final conditions [18]. On the other hand, direct MS breaks the problem into shorter steps [18], greatly enhancing the robustness of the shooting method, at the cost of having a larger number of variables. It is then primordial to exploit matrix sparsity to efficiently solve the NLP equations. An additional difficulty exists with the shooting techniques, namely the necessity of defining constrained and unconstrained subarcs a priori, when solving problems with path inequality constraints [18]. This issue however does not exist with SCP methods. In the realm of direct SCP, Global Orthogonal Approaches (GOA), or spectral methods, have received much attention in the last decade, since they have the advantage of providing exponential convergence, for the approximation of analytic functions. This is an important aspect since the efficiency and even convergence of NLPs improves for a problem of smaller size. In a GOA, the state vector is expressed as a truncated series expansion

$$\mathbf{x}(t) \approx \mathbf{x}_M(t) = \sum_{k=1}^M \mathbf{a}_k \cdot \mathcal{O}_k(t) \quad t \in \Omega = (T_o, T_f) \quad (10)$$

characterized by the *trial* functions $\mathcal{O}_k(t)$, or Basis (BA), and \mathbf{a}_k the Expansion Coefficients (EC) determined from *test* functions, which attempt to ensure that the (ODEs) are optimally satisfied. The choice of BA is what distinguishes GOA methods from finite-difference or finite-element methods. In both finite-type methods, the BA is local in character, while for GOA methods the BA consists of infinitely differentiable global functions, such as orthogonal polynomials or trigonometric functions [19]. Further, the EC distinguish the three most common types of GOA methods, namely Galerkin, Tau, and collocation. In the sequel, and due to space limitations, we only briefly review the GOA collocation method, or pseudospectral, used for the discretization of our continuous-time problem. In the collocation approach, the EC are Dirac delta functions centered at M support points P_k , defined by the set $\mathcal{C} = \{P_k | k \in \{1, \dots, M\}\}$. The EC are determined s.t. (i) the boundary conditions (3) are met, and (ii) the (ODEs) given by (2) are exactly satisfied on \mathcal{C} by

$$\dot{\mathbf{x}}_M(t_k) - f(\mathbf{x}(t_k), \mathbf{u}(t_k), t_k) = 0 \quad \forall k \in \{1, \dots, M\} \quad (11)$$

In addition, the BA is described on \mathcal{C} by Lagrange interpolating polynomials $L_k(\tau)$ [20], s.t.

$$\begin{aligned} \mathbf{x}_M(\tau) &= \sum_{k=1}^M \mathbf{a}_k \cdot L_k(\tau) \\ L_k(\tau) &\triangleq \prod_{j=1, j \neq k}^M \frac{\tau - \tau_j}{\tau_k - \tau_j} = \frac{h(\tau)}{(\tau - \tau_k) \frac{d}{d\tau} h(\tau)} \end{aligned} \quad (12)$$

where the time variable t has been mapped to the pseudospectral interval $\tau \in [-1, 1]$, via the affine transformation $\tau = \frac{2t}{T_f - T_o} - \frac{T_f + T_o}{T_f - T_o}$. We also define $h(\tau) = (1 + \tau) \cdot P_M(\tau)$ [21], where $P_M(\tau)$ is often related to Legendre or Chebyshev

polynomials. In our case, we use a M^{th} -degree Legendre polynomial given by

$$P_M(\tau) \triangleq \frac{1}{2^M M!} \frac{d^M}{d\tau^M} [(\tau^2 - 1)^M] \quad (13)$$

Note that Lagrange polynomials are helpful for collocation; it is straightforward to show that $\forall k \in \{1, \dots, M\}$

$$L_k(\tau_j) = \delta_{kj} = \begin{cases} 1 & k = j \\ 0 & k \neq j \end{cases} \quad (14)$$

Hence $\mathbf{x}_M(\tau_k) = \mathbf{a}_k$ on \mathcal{C} , satisfying (11). In a similar way, the input control vector is approximated with a basis of Lagrange polynomials, although not necessarily identical to the previous ones. Besides the choice of \mathcal{C} , another set of K points Q_k , defined by $\Omega = \{Q_k | k \in \{1, \dots, K\}\}$, is required for the discretization of the cost functional (1) and the (ODEs) in (2). Here Ω is chosen s.t. the quadrature approximation of an integral is minimized. We have

$$\int_{-1}^1 g(\tau) d\tau \approx \sum_{k=1}^K w_k \cdot f(\tau_k) \quad \tau \in [-1, 1] \quad (15)$$

with w_k the quadrature weights. Now, it is well known that the highest accuracy quadrature approximation, for a given Ω , is the Gauss quadrature. In this case, Ω is defined by the roots of a K^{th} -degree Legendre polynomial $P_K(\tau)$, where the corresponding Gauss weights w_k are given from [20] as

$$w_k \triangleq \frac{2}{(1 - \tau_k^2) \left(\frac{dP_K(\tau_k)}{d\tau} \right)^2} \quad \forall k \in \{1, \dots, K\} \quad (16)$$

IV. SIMULATION RESULTS

The simulation software uses the helicopter UAV flight dynamics model, presented in Section II, and implemented in MATLAB[®], for the case of a small-scale helicopter UAV with a mass of 8.35 kg and a rotor diameter of 1.87 m. Further, the pseudospectral discretization method is made available in a MATLAB environment, through the open-source General Pseudospectral Optimal control Software GPOPS[®]. The optimal control problem must first be reformulated into a GPOPS format, as a set of m-files [22], and the model must be expressed in a vectorized structure. Once discretized, our problem is then transcribed into a large-scale, static, sparse, and finite-dimensional NLP optimization problem. To solve this NLP, we use SNOPT[®], a SQP based solver. The simulations are set to compare our cost functional to costs from previous research, as outlined in Section I, see Table I, with the following initial conditions: steady-state hover, at 40 m altitude, and in a zero-wind environment. In these examples, the discretization of the optimal problem uses 29 nodes, yielding a NLP having 607 variables and 534 constraints. Further, finite differencing has been used to estimate the objective gradient and constraint Jacobian. In this case, the computational time for a single trajectory, on a legacy computer hardware, is in the range of one to two hours. Here for the analysis of each cost $J_j, \forall j \in \{1, \dots, 4\}$, we consider the following power metric $P_{ij}, \forall i \in$

$\{1, 2, 3\}$, of the vector-valued discrete-time signal $z_i(n)$, s.t. $z_1(n) \in l_2([1, N_j], \mathbb{R}^4)$, $z_2(n) \in l_2([1, N_j], \mathbb{R}^3)$, $z_3(n) \in l_2([1, N_j], \mathbb{R}^2)$, $\forall n \in \{1, \dots, N_j\}$, $N_j \in \mathbb{Z}^+$, with

$$\begin{aligned} P_{ij} &:= \frac{1}{N_j} \|z_i(n)\|_{l_2}^2 = \frac{1}{N_j} \sum_{n=1}^{n=N_j} \|z_i(n)\|_2^2 \\ z_1(n) &= (\dot{\theta}(n)_0 \quad \dot{\theta}(n)_{TR} \quad \dot{\theta}(n)_{1c} \quad \dot{\theta}(n)_{1s})^T \\ z_2(n) &= (u(n) \quad v(n) \quad w(n))^T \\ z_3(n) &= (v(n) \quad \phi(n))^T \end{aligned} \quad (17)$$

Where we use the norm on the square-summable sequence space l_2 , the discrete-time equivalent of the continuous-time space L_2 . For each test case, these signal power metrics are reported in Table II. First, Fig. 2 and Fig. 3 show the input control rate activity, where the magenta horizontal lines display hard bounds on model variables. We clearly see that test cases J_1 and J_3 display the lowest level of activity, confirmed by the power values $P_{11} = 0.13$ and $P_{13} = 0.23$, since both costs include the input rates. Further, if a running cost over time J_4 is to be used, versus a final-time only cost J_2 , then minimization of control rates ought to be included. Indeed we have $P_{14} = 3.27$ much higher than $P_{12} = 0.28$. We also note that control rate minimization comes at the expense of a higher vehicle longitudinal velocity u during flight, see Fig. 6, compare (P_{21}, P_{23}) to (P_{22}, P_{24}) . Although lower kinetic energy during the descent is desirable, since this simplifies the final landing maneuver, excluding the control rates from the cost functional is an even worse alternative, since this may lead to the excitation of unmodeled or undesirable high frequency modes, potentially resulting in closed-loop instability. This matter is particularly relevant, when the subsequent synthesis of a feedback controller is based upon low-order model representations. Next, from Fig. 4 we see the MR collective θ_0 going full-down, as soon as the maneuver initiates. As expected, this is necessary in order to minimize main rotor RPM decay. Besides, θ_0 sharply increases as the helicopter nears to the ground, to prevent rotor over-speed, while reducing the sink rate. We also note the gradual change of tail rotor collective θ_{TR} , for J_1 and J_3 , in accordance with control rate minimization. From Fig. 5, we see that our cost functional considerably reduces lateral control activity θ_{1c} . This is also supported by the negligible sideways velocity v , achieved by our cost objective, see Fig. 6, and compare also P_{31} to (P_{32}, P_{33}, P_{34}) . The benefits of reduced lateral motion are increased flight performance, and decreased roll-yaw coupling. Further in our case, the longitudinal cyclic θ_{1s} is mainly used to (i) manage vehicle and main rotor kinetic energies, (ii) reduce forward airspeed, and (iii) level the attitude for a proper landing, see Fig. 5. Finally, Fig. 7 presents the 3-D inertial position. Again, lateral displacement is minimal in our case. We note also that the use of a final-time only cost, such as J_2 , tends to increase the traveled distance and flight time.

V. CONCLUSION

Through a direct optimal control framework, we derive optimal power-off landing trajectories, for the case of a

TABLE I
TEST CASES: COST FUNCTIONALS

Test Case	Cost Functional	Line Color & Style in Figures
J_1	Our definition as given in (7)	Red (solid line)
J_2	$J := \Phi(\mathbf{x}(T_f), T_f)$ $= u(T_f)^2 + v(T_f)^2 + w(T_f)^2$ $+ p(T_f)^2 + q(T_f)^2 + r(T_f)^2$ $+ \phi(T_f)^2 + \theta(T_f)^2$	Black (dotted line)
J_3	$J := \int_{\Omega} \Psi(\mathbf{u}(t)) dt$ $= \int_{\Omega} (\dot{\theta}_0^2 + \dot{\theta}_{TR}^2 + \dot{\theta}_{1c}^2 + \dot{\theta}_{1s}^2) dt$	Green (dashed line)
J_4	$J := \int_{\Omega} \Psi(\mathbf{x}(t)) dt$ $= \int_{\Omega} [(\Omega_{MR} - \Omega_{MR100\%})^2 + (u^2 + w^2)] dt$	Blue (dashed-dotted line)

TABLE II
TEST CASES: SIGNAL POWERS

Test Case	Control rates P_{1j}	3-D linear motion P_{2j}	Lateral motion P_{3j}
J_1	0.13	163	0.1
J_2	0.28	89	6.7
J_3	0.23	171.7	11.8
J_4	3.27	140.5	14.5

small-scale helicopter UAV. These open-loop optimal trajectories, generated by a Trajectory Planner (TP), represent the solution to the minimization of a cost objective, given system dynamics, controls and states equality and inequality constraints. Our cost objective maximizes flight performance and control smoothness, while minimizing roll-yaw coupling, hence lowering the workload of any feedback Trajectory Tracker (TT) controller. Additionally, our direct method provides exponential convergence, implying increased computational efficiency, provided the functions under considerations are sufficiently smooth. Hence, for a range of initial conditions, optimal autorotative trajectories can be computed off-line by a TP, and stored as lookup tables, on-board a flight control computer. By so doing, these trajectories provide both the optimal states to be tracked by a TT, and the feedforward nominal controls to track the trajectory. In this case, it would particularly be interesting to analyze the robustness of the obtained trajectories, with respect to model uncertainties, i.e. unmodeled higher-order dynamics, unmodeled static nonlinearities, and parametric uncertainties. Although results on static robust optimization have been proven, the field of (dynamic) robust optimization, for high-order systems, is still in its infancy. Another extension concerns the robustness of the obtained trajectories, with respect to signal uncertainties, i.e. wind disturbances and signal noise; problems at the heart of stochastic optimization. Finally, each new helicopter configuration, modifying main rotor inertia or vehicle weight, may likely result in distinct optimal solutions. In order to limit the on-board memory requirement, i.e. the storage of a large family of optimal reference trajectories, it would be beneficial to express these optimal solutions in a non-dimensional form, independent of specific helicopter configurations. These aspects, together with the design of a TT, have been identified as topics for future research.

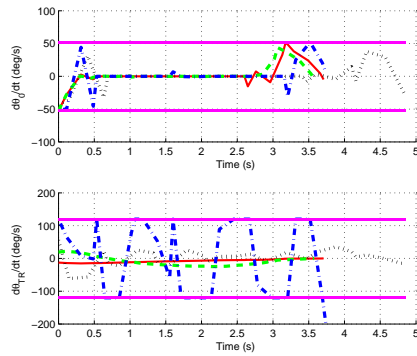


Fig. 2. MR & TR Collective Control Input Rates

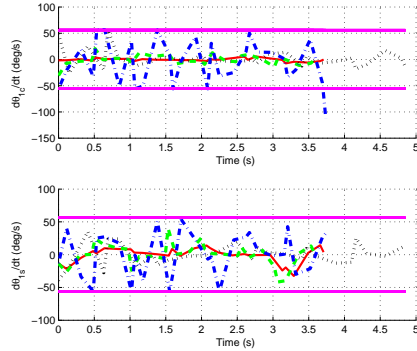


Fig. 3. MR Lat./Long. Cyclic Control Input Rates

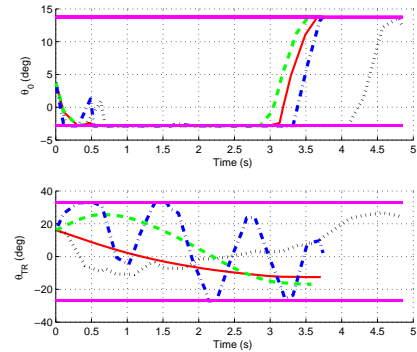


Fig. 4. MR & TR Collective Control Inputs

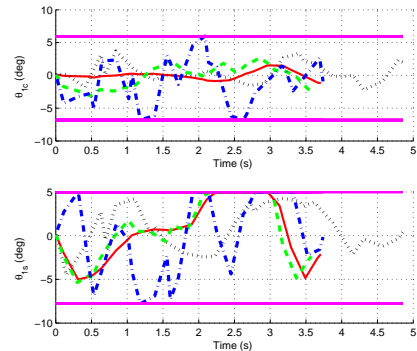


Fig. 5. MR Lat./Long. Cyclic Control Inputs

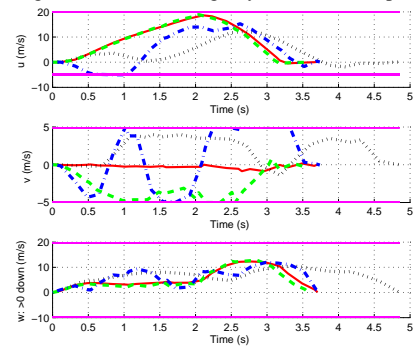


Fig. 6. Vehicle Body Linear Velocities

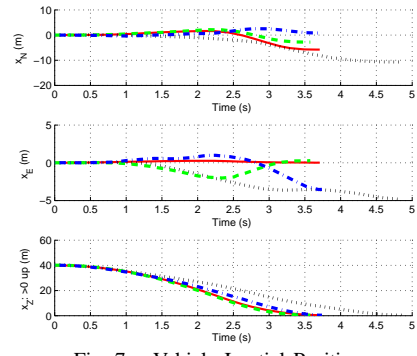


Fig. 7. Vehicle Inertial Position

REFERENCES

- [1] P. Abbeel, A. Coates, T. Hunter, and A. Y. Ng, "Autonomous autorotation of an rc helicopter," in *11th International Symposium on Experimental Robotics (ISER)*, 2008.
- [2] W. Johnson, "Helicopter optimal descent and landing after power loss," NASA Ames Research Center, Tech. Rep. TM 73-244, 1977.
- [3] A. Y. Lee, A. E. Bryson, and W. S. Hindson, "Optimal landing of a helicopter in autorotation," *AIAA Journal of Guidance, Control, and Dynamics*, vol. 11, no. 1, pp. 7–12, 1988.
- [4] M. W. Floros, "Descent analysis for rotorcraft survivability with power loss," in *65th Forum of the American Helicopter Society*, 2009.
- [5] A. A. Jhemi, E. B. Carlson, Y. J. Zhao, and R. T. N. Chen, "Optimization of rotorcraft flight following engine failure," *Journal of the American Helicopter Society*, 2004.
- [6] B. L. Aponso, E. N. Bachelder, and D. Lee, "Automated autorotation for unmanned rotorcraft recovery," in *AHS International Specialists' Meeting On Unmanned Rotorcraft*, 2005.
- [7] P. Bibik and J. Narkiewicz, "Helicopter modeling and optimal control in autorotation," in *Forum of the American Helicopter Society*, 2008.
- [8] C. L. Bottasso, G. Maisano, and F. Scorcelletti, "Trajectory optimization procedures for rotorcraft vehicles, their software implementation, and applicability to models of increasing complexity," *Journal of the American Helicopter Society*, 2010.
- [9] K. Dalamagkidis, K. P. Valavanis, and L. A. Piegl, "Autonomous autorotation of unmanned rotorcraft using nonlinear model predictive control," *Journal of Intelligent and Robotic Systems*, vol. 57, p. 351369, 2010.
- [10] S. Tierney and J. W. Langelaan, "Autorotation path planning using backwards reachable set and optimal control," in *66th Annual Forum of the American Helicopter Society*, 2010.
- [11] J. Holsten, S. Loechelt, and W. Alles, "Autonomous autorotation flights of helicopter uavs to known landing sites," in *66th Annual Forum of the American Helicopter Society*, 2010.
- [12] T. Yomchinda, J. F. Horn, and J. W. Langelaan, "Flight path planning for descent-phase helicopter autorotation," in *AIAA Guidance, Navigation, and Control Conference*, 2011.
- [13] A. E. Bryson and Y. C. Ho, *Applied Optimal Control*. New York: Taylor & Francis Group, 1975.
- [14] S. Taamallah, "Flight dynamics modeling for a small-scale flybarless helicopter uav," in *AIAA Atmospheric Flight Mechanics Conference*, 2011.
- [15] H. B. Keller, "Numerical solution of two point boundary value problems," *SIAM*, 1976.
- [16] H. G. Bock and K. J. Plitt, "A multiple shooting algorithm for direct solution of optimal control problems," in *IFAC 9th W.C.*, 1984.
- [17] L. T. Biegler, "An overview of simultaneous strategies for dynamic optimization," *Chemical Engineering and Processing: Process Intensification*, vol. 46, no. 11, pp. 1043–1053, 2007.
- [18] J. T. Betts, "Practical methods for optimal control using nonlinear programming," in *SIAM*, 2001.
- [19] B. Fornberg, *A Practical Guide to Pseudospectral Methods*. Cambridge University Press, 1998.
- [20] P. J. Davis and P. Rabinowitz, *Methods of Numerical Integration*. Dover Publications, 2007.
- [21] G. T. Huntington, "Advancement and analysis of a gauss pseudospectral transcription for optimal control," Ph.D. dissertation, Massachusetts Institute of Technology, 2007.
- [22] A. V. Rao, D. A. Benson, C. Darby, M. A. Patterson, C. Franconlin, I. Sanders, and G. T. Huntington, "Algorithm xxx: Gpops, a matlab software for solving multiple-phase optimal control problems using the gauss pseudospectral method," ACM Inc., Tech. Rep., 2008.